

# Molecular structure, electric property, and scintillation and quenching of liquid scintillators

Zhe Wang,<sup>1,2,3,\*</sup> Ye Liang,<sup>1,2,3</sup> and Haozhe Sun<sup>1,2,3</sup>

<sup>1</sup>*Department of Engineering Physics, Tsinghua University, Beijing 100084, China*

<sup>2</sup>*Center for High Energy Physics, Tsinghua University, Beijing 100084, China*

<sup>3</sup>*Key Laboratory of Particle & Radiation Imaging (Tsinghua University), Ministry of Education, Beijing 100084, China*

(Dated: August 28, 2025)

Liquid scintillators are widely used in particle and nuclear physics. Understanding the scintillation and quenching mechanisms is a fundamental issue in designing a high-light-yield liquid scintillator. In this work, the basic scintillation process for a two-component liquid scintillator is reviewed, highlighting the processes of excitation, ionization, anion-cation recombination, and electric dipole-dipole energy transfer. A molecule's polar group, polarization characteristics, and the corresponding material's dielectric constant are found to be correlated with a liquid scintillator's scintillation efficiency. Polar groups and high relative dielectric constants (permittivity values) can cause severe quenching and should be avoided. The tellurium loading scheme in the liquid scintillator of the SNO+ experiment, TeBD, is discussed. The hydroxyl groups introduce polar structures in the TeBD, and the relative dielectric constant of our reproduced sample is measured to be  $17 \pm 2$ . These discussions explain part of the quenching of the TeBD liquid scintillator.

Keywords: liquid scintillator, dielectric constant, polar group, quenching, tellurium

## I. INTRODUCTION AND MOTIVATION

Liquid scintillators are widely used in particle and nuclear physics. They are also powerful research tools in chemistry, biology, medicine, etc. To develop a high-light-yield liquid scintillator is difficult [1, 2], in particular, with a specific isotope loading for various purposes. For instance, people are testing several tellurium loading schemes for the neutrinoless double beta decay study [3–8] and are looking for an ideal approach.

For a liquid scintillator design, an understanding of the scintillation and quenching mechanism is expected. But, unfortunately, there is no complete theory or model to explain the relation between the light yield performance and the structure of the involved molecules. For instance, we have been trying to develop a water-based liquid scintillator [9], expecting a lower budget and a better solubility with inorganic salt [8]. Phenol and benzyl alcohol have been chosen to be mixed with water because they both have scintillation groups, benzene rings, and hydrophilic groups, hydroxyls (-OH). But the system does not show an equal amount of light yield as scaled from the linear alkylbenzene (LAB) based liquid scintillator. The various tellurium loading plans [3–8] also show different light yield performance. We hope to understand the reason from the bottom and to accelerate the liquid scintillator development.

This work discusses part of this critical issue, focusing on the electric property of a liquid scintillator. The electric polar groups and polarization characteristics of liquid scintillator molecules play an important role in

the scintillation and quenching process. The related dielectric constant, also called permittivity, should be measured and is worth noting.

The paper is presented in the following way. In Sec. II, the scintillation process is reviewed, including the energy deposition process of charge particles and the energy transfer process between molecules. This section will highlight the processes of anion-cation recombination and electric dipole-dipole energy transfer. In Sec. III, the electric property-related quenching effect is explained, focusing on the impact of polar groups and dielectric constant on the anion-cation recombination and the electric dipole-dipole energy transfer. In Sec. IV, the tellurium loading scheme of the SNO+ experiment [3] is investigated. The electric property of the synthesis product is measured. Then, in Sec. V, the connection between the molecular structure, electric property, and scintillation and quenching issues is summarized.

## II. SCINTILLATION PROCESS

This paper is about the binary liquid scintillator system, for instance, LAB with 2,5-diphenyloxazole (PPO), in which LAB is the solvent and dominant in mass, and PPO is only at the level of a few grams per liter. LAB is the primary scintillation component, and PPO is the secondary component. The primary component absorbs almost all of the energy deposited by radiation and can emit short-wavelength scintillation light or transfer its excitation state energy to the secondary component. With the received energy, the secondary component emits longer wavelength scintillation light for a higher propagation length and for a higher quantum efficiency of an optical photon instrument, for instance, a photomultiplier tube. The

---

\*Corresponding author: wangzhe-hep@mail.tsinghua.edu.cn

process is presented in Fig. 1, where D is for the primary component, donor or solvent, and A is for the secondary component, acceptor or solute. The details are presented below.

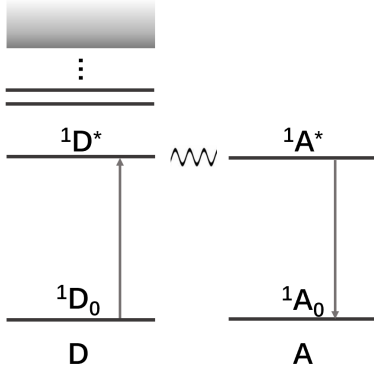


FIG. 1: A simplified schematic diagram of the scintillation process. D is for the primary component, donor or solvent, and A is for the secondary component, acceptor or solute. More explanations are in the text.

### A. Energy deposit of charged particles

Elastic scattering, excitation, and ionization are the major physics processes of a charged particle with liquid scintillator molecules. As presented in Fig. 1, solvent molecules are excited from their ground states,  $^1D_0$ , to their excited states, represented by the horizontal solid lines above,  $^1D^*$ . Here the post-script 0 and \* refer to the ground and excited states, respectively. The pre-script, 1, refers to the spin singlet. If the absorbed energy is very high, electrons are released, and anions and cations are created in the liquid. This transition from the higher and continuous excited states to free electron release is represented by the gray-to-white area in the figure. Anions (electrons) and cations, and excited states are the major products after ionization and excitation processes.

Some of the electrons and cations can recombine into neutral excited states, while some electrons can be dissolved in the solvent and cannot finally contribute back to scintillation. The recombination rate will increase with a higher attraction force between the positive and negative charges and the media, which is governed by Coulomb's Law.

$$F = \frac{1}{4\pi\epsilon_0\epsilon} \frac{q_1 q_2}{r^2}, \quad (1)$$

where  $q_1$  and  $q_2$  are the charge of an electron and a cation, respectively,  $\epsilon_0$  is the dielectric constant or permittivity of vacuum,  $\epsilon$  is the relative dielectric constant of the medium, and  $r$  is their distance. On the other hand, the electrophilic characteristics of some solvent molecules will facilitate the electron solvation.

### B. Energy transfer

The energy is transferred from the solvent molecule's excited states,  $^1D^*$ , to the second component, A, as in Fig. 1, and A is excited from  $^1A_0$  to  $^1A^*$ . The deexcitation of  $^1A^*$  gives the scintillation lights. The energy transition is conducted dominantly by two mechanisms. The first one is the Föster resonance energy transfer (FRET), i.e., electric dipole-dipole interaction [10]. The second one is the charge exchange effect [11].

The FRET mechanism is known as non-radioactive long-range energy transfer. From the point of view of quantum electrodynamics, the FRET is mediated by a virtual photon, which is presented as a wavy line in Fig. 1. The theoretical description of FRET is the electric dipole-dipole interaction. The static electric energy,  $W$ , is

$$W = \frac{1}{4\pi\epsilon_0\epsilon R^3} \left[ \vec{m}_1 \cdot \vec{m}_2 - 3 \frac{(\vec{m}_1 \cdot \vec{R})(\vec{m}_2 \cdot \vec{R})}{R^2} \right], \quad (2)$$

where the  $\epsilon_0$  and  $\epsilon$  are the same as in Eq. 1,  $\vec{R}$  is the distance vector between D and A,  $R$  is its absolute value, and  $\vec{m}_1$  and  $\vec{m}_2$  are the electric dipole vectors of D and A's first excited states. The energy  $W$  is proportional to the reciprocal of the relative dielectric constant.

When calculating the FRET transition rate,  $W$  goes into the Hamiltonian, and the transition rate is proportional to the reciprocal of the relative dielectric constant squared. The rate,  $k$ , is expressed as [12]

$$k = \frac{9000(\ln 10)\kappa^2\Phi_D^0}{128\pi^5 n^4 N \tau R^6} \int f_a(\tilde{\nu})\epsilon_b(\tilde{\nu}) \frac{d\tilde{\nu}}{\tilde{\nu}^4}, \quad (3)$$

where  $\kappa$  is the orientation factor between the donor and acceptor dipole vectors,  $\Phi_D^0$  is the quantum yield of the donor in the absence of the acceptor,  $n$  is the refractive index of the medium through which the energy transfer occurs,  $N$  is the Avogadro's number,  $\tau$  is the lifetime of the donor in the absence of the acceptor,  $R$  is the same as in Eq. 2,  $f_a(\tilde{\nu})d\tilde{\nu}$  is the normalized fluorescence of the donor in the wavenumber range of  $\tilde{\nu}$  to  $\tilde{\nu}+d\tilde{\nu}$ ,  $\epsilon_b(\tilde{\nu})$  is the absorption coefficient of the acceptor at the wave number  $\tilde{\nu}$ . The dependence on  $1/\epsilon^2$  is hidden in  $n$  ( $n = \sqrt{\epsilon\mu}$ ), where  $\mu$  is the relative magnetic permeability.

The charge exchange energy transfer [11] is a short-range energy transfer, which relies on the wavefunction overlap of the electronic states between different molecules. The details of it are not the focus of this work and will be skipped.

### III. ELECTRIC PROPERTY RELATED QUENCHING

#### A. Quenching in anion-cation recombination

Liquid scintillator molecules' polar groups, their polarization characteristics, and the related dielectric constant of the whole liquid can seriously affect the anion-cation recombination. There can be a quantitative connection between the recombination probability with the structures and the relative dielectric constant.

The yield of free ions by radiation has been thoroughly investigated in the past [13]. After ionization, usually an electron will return to its parent ion and go back to an excited state, contributing scintillation, but some electrons will escape from the initial recombination. The number of escaped electrons per unit energy input by radiation is called the free ion yield.

The escaped electrons can be quasi-free electrons in a delocalized state in a conduction band, or aggregate with solvent molecules to form a solvated electron. With a lot of polar groups, a high dielectric constant is granted. As expressed in Eq. 1, the recombination attraction force is proportional to the reciprocal of the dielectric constant.

Water has a relative dielectric constant of 78.36 at 0 Hz at 25 °C [14]. As a comparison, the relative dielectric constants for benzene, toluene, *p*-xylene, ethylbenzene, propylbenzene, and butylbenzene at 0 MHz and 20 °C are 2.28, 2.38, 2.27, 2.45, 2.37, and 2.36, respectively [14]. The relative dielectric constant of LAB should be in this range, too. It is assumed to be 2.5 in this work.

The relative dielectric constant varies with frequency and temperature, since medium's molecules cannot respond instantly to high frequency external field. Higher temperature will induce smaller viscosity and faster response to the external field. The real part of water's relative dielectric constant is in the range of 78 - 15 for the frequency range of 0 Hz - 50 GHz at 25 °C [14]. For anion-cation recombination, the lifetime of free electrons can be extremely short and is in the ps range. Currently, no detailed results for popular organic liquids and water are found, so we chose their values at 0 Hz as a proxy.

With the information compiled in Ref. [13], the free ion yields of all organic molecules, including oxygen atom, i.e., ether, alcohol, ketone, and ester, are plotted with their relative dielectric constants in Fig. 2. Water and four aromatic molecules, similar to LAB, are also plotted for comparison. The data points lie in the diagonal region and are coarsely correlated. For water, the free ion yield is 2.7/100 eV [13].

In order to understand the importance of the combination of positive and negative ions, we compared the yield of free ions to the yield of excited states or to the yield of all electrons.

With the Geant4-DNA package [15–22], keV electrons are simulated in water with option 4, and the numbers of total ionization electrons and excited states are counted, where no recombination is simulated. The yields of total

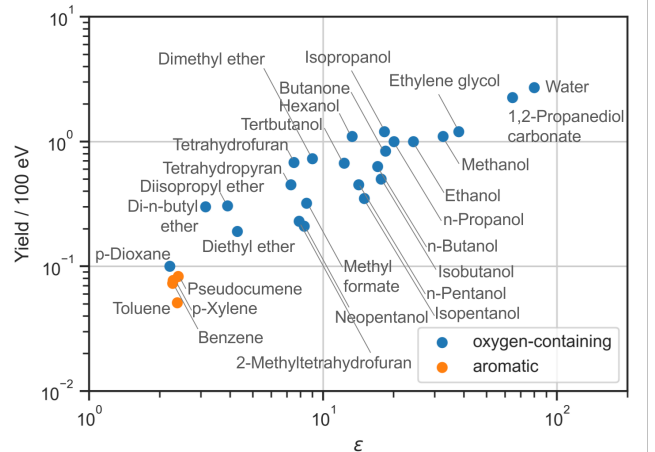


FIG. 2: Free ion yield with relative dielectric constant. [13].

electrons and excited states are 4.4/100 eV and 2.3/100 eV, respectively. We see that the free ion yield 2.7/100 eV is quite significant and takes about  $2.7/(4.4+2.3) = 40\%$ .

With the same Geant4-DNA package, we adjusted several configurations for benzene simulation. The ionization, excitation, and elastic scattering cross-sections for water are replaced with the cross-sections for benzene with the data given in Ref. [23]. The angular differential cross-section for ionization is set with Ref. [24]. With the simulation of 1 keV electrons, the yields of total electrons and excited states are 5.6/100 eV and 6.0/100 eV. The results are slightly higher than in water due to smaller excitation and ionization thresholds and higher cross-sections.

#### B. Quenching in electric dipole-dipole Energy transfer

As explained in Sec. II B, Eq. 3, the electric dipole-dipole transition rate is proportional to  $1/n^4$ , i.e.,  $1/(\epsilon^2 \mu^2)$ . Most materials involved in liquid scintillation production are diamagnetic, and their magnetic permeability values are about 1, unless  $O_2$  or organic molecules with free radicals are involved. But their relative dielectric constants are quite different.

The relative dielectric constant changes with temperature and frequency. The value will be more appropriate if it corresponds to the frequency of a liquid scintillator, i.e., the reciprocal of its lifetime, for instance, at 100 MHz - 1 GHz for LAB [25, 26] and at the right temperature. The relative dielectric constant of water in this range is about 80 [14]. At the same time, we still take the approximate value of LAB of 2.5 as in Sec. III A. The electric dipole-dipole energy transfer rate in water is about 1000 times weaker than in LAB.

## IV. ELECTRIC PROPERTIES OF TeBD AND QUENCHING

### A. Synthesis of TeBD

Following the procedure of tellurium loading of the SNO+ experiment [3], we synthesized a chemical with telluric acid, TeA, and 1,2-butanediol, BD, and the final product is called TeBD. The product is similar to the SNO+ publication, but not identical, and the detail is explained below. TeA with purity over 98% was ordered from Shanghai Macklin Biochemical Technology Co., Ltd. BD with purity over 99% was ordered from Beijing Konosience Technology Ltd. No further purification is applied. TeA aqueous solution and BD were mixed with a molar ratio of TeA to BD of 3:1. The mixture was heated and agitated continuously under vacuum to remove water at 70 - 80 °C. The heating was applied until the product reached the solubility point in LAB.

Before the sample was analyzed with an LCMS-IT/TOF Mass Spectrometer, Shimadzu Japan, the sample was sealed and stored in our laboratory for a few weeks; however, with inevitable contact with air and the vapor in air. The analysis result is shown in Fig. 3 and Fig. 4 for positive and negative modes, respectively. No additional two hours of heating was conducted before the mass spectrometer analysis, as in Ref. [3].

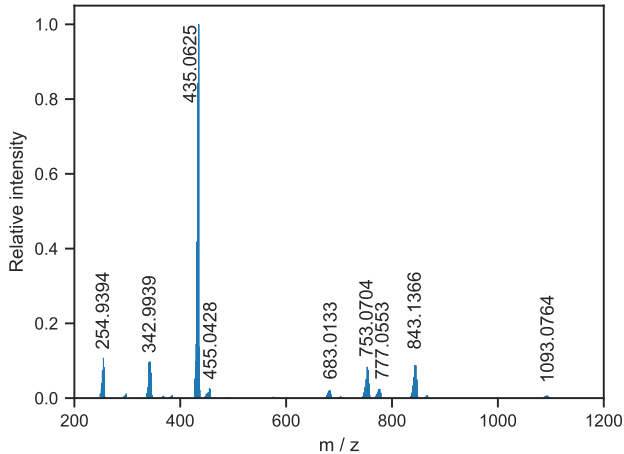


FIG. 3: Positive ion mass spectrum for TeBD.

With these analysis results, the major TeBD products are identified as in Ref. [3]. The structure b in Fig. 4 of Ref. [3] is visible on the peak 435 in positive mode figure and peak 411 in the negative mode figure. This is the major product of our TeBD mixture product, and its structure, as suggested by Ref. [3], is replotted in Fig. 5. Note that in the positive mode, peak positions are possible to be shifted by adding the contribution of hydrogen or by sodium contamination, i.e. be shifted by their mass number 1 or 24, respectively, which is an intrinsic feature of the mass spectrometer. The structure

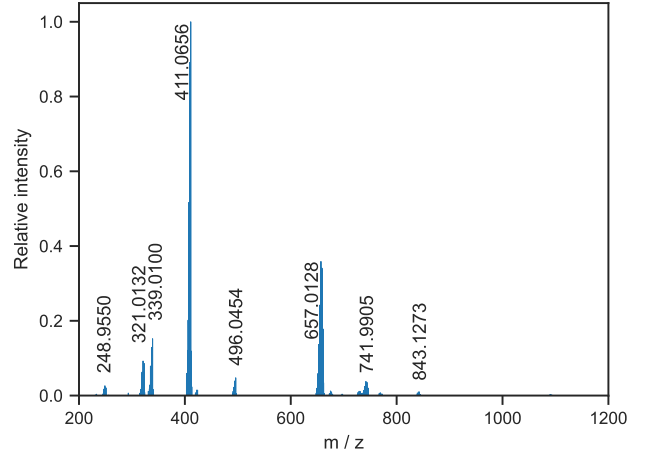


FIG. 4: Negative ion mass spectrum for TeBD.

d in Fig. 4 of Ref. [3], which is the major product of SNO+ TeBD can be seen on peak 753 in the positive mode figure with a mass of 729, if subtracting 24. Its structure is shown in Fig. 6 [3]. The structure a in Fig. 4 of Ref. [3] is visible on peak 342 in the positive mode and peak 339 in the negative mode. The structure c in Fig. 4 of Ref. [3] is visible on peak 657 in the negative mode. The structure e in Fig. 4 of Ref. [3] is visible on peak 843 in the positive mode, if subtracting 24. The major difference with Ref. [3] is that our sample was not heated beyond the LAB solubility point and had contact with vapor, so there is much less further oligomerisation in our sample.

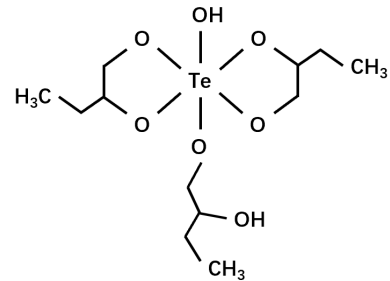


FIG. 5: Molecule structure TeBD at mass 411, which is the dominant synthesis product of this work.

### B. Electric property of TeBD

#### 1. Polar groups in TeBD

There are two hydroxyl groups in each TeBD composition, as shown in Fig. 5 and 6, one can expect they have similar effects on anions and cations as other alcohol substances. These polar groups can slow down

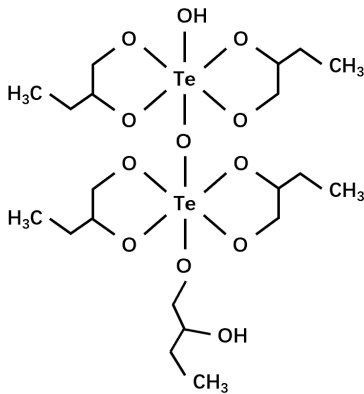


FIG. 6: Molecule structure TeBD at mass 729, which is the dominant synthesis product of Ref. [3].

and prevent some of the anion-cation recombination back to excited states for scintillation and can cause quenching.

## 2. Dielectric constant of TeBD

The relative dielectric constant of TeBD of this work was measured with a dielectric constant and dielectric loss testing instrument, mode DHGTJS, produced by Shanghai Donghai Electric CO., LTD.

We first measured the relative dielectric constants of ethanol and cyclohexane at 1 MHz and 28 °C. The frequency was limited by our instrument. The temperature was our room temperature. The results of ethanol are in the range of 25.9-27.4 for ethanol and the reported result is 25.3 at 0 Hz and 20 °C [14]. The results of cyclohexane are measured around 1.12 and the reported result is 2.02 at 0 Hz and 20 °C [14]. These results basically verified the reliability of the instrument and gave the systematic uncertainty.

The result of the TeBD sample of this work is measured

to be  $17 \pm 2$  at 1 MHz and 28 °C.

If we take the relative dielectric constant of LAB as 2.5, then the ratio of TeBD to LAB is 6.84, and the electric dipole-dipole energy transfer rate in pure TeBD is 47 times weaker than LAB. This also partially explains what caused the quenching of TeBD.

## V. SUMMARY

In this paper, the energy deposition and scintillation processes in two-component liquid scintillators are briefly reviewed, and the key features in anion-cation recombination and electric dipole-dipole energy transfer are pointed out. Polar groups and a high dielectric constant of a liquid scintillator can slow down or prevent some of the anion-cation recombination and reduce scintillation. A high dielectric constant is also directly responsible for the energy transfer rate from donor to acceptor, according to the function of  $1/\epsilon^2$ . The cases of water and TeBD are discussed and analyzed in this work. The relative dielectric constant of TeBD is measured to be  $17 \pm 2$ . Hopefully, some new chemicals and molecular structures can be identified in the future with fewer polar groups and a low dielectric constant to reach a higher scintillation light yield.

## Acknowledgments

This work is supported in part by the National Natural Science Foundation of China (No. 12141503), the Ministry of Science and Technology of China (No. 2022YFA1604704), the Key Laboratory of Particle & Radiation Imaging (Tsinghua University), and the CAS Center for Excellence in Particle Physics (CCEPP). I also like to thank Minfang Yeh for helping me to digest many chemical concepts.

- 
- [1] M. R. Anderson et al. Development, characterisation, and deployment of the SNO+ liquid scintillator. *JINST*, 16(05):P05009, 2021.
  - [2] Christian Buck and Minfang Yeh. Metal-loaded organic scintillators for neutrino physics. *J. Phys. G*, 43(9):093001, 2016.
  - [3] D. J. Auty et al. A method to load tellurium in liquid scintillator for the study of neutrinoless double beta decay. *Nucl. Instrum. Meth. A*, 1051:168204, 2023.
  - [4] I. A. Suslov, I. B. Nemchenok, Yu. A. Shitov, S. V. Kazartsev, V. V. Belov, and A. D. Bystryakov. Development of a new tellurium loaded liquid scintillator based on linear alkylbenzene. *Nucl. Instrum. Meth. A*, 1040:167131, 2022.
  - [5] I. Suslov, I. Nemchenok, and A. Bystryakov. A novel approach to load tellurium in liquid scintillator. *JINST*, 20(04):P04032, 2025.
  - [6] I. Suslov, I. Nemchenok, A. Klimenko, A. Bystryakov, and I. Kamnev. Tellurium-loaded organic scintillators. *JINST*, 18(08):P08026, 2023.
  - [7] Ya-Yun Ding, Meng-Chao Liu, Liang-Jian Wen, Yuan-xia Li, Gao-song Li, and Zhi-yong Zhang. A novel approach in synthesizing Te-diol compounds for tellurium-loaded liquid scintillator. *Nucl. Instrum. Meth. A*, 1049:168111, 2023.
  - [8] Ye Liang, Haozhe Sun, and Zhe Wang. A new tellurium-loaded liquid scintillator based on p-dioxane. 5 2025.
  - [9] M. Yeh et al. A new water-based liquid scintillator and potential applications. *Nucl. Instrum. Meth. A*, 660:51–56, 2011.
  - [10] Th. Förster. Zwischenmolekulare Energiewanderung und

- Fluoreszenz. *Annalen Phys.*, 437(1-2):55, 1948.
- [11] D. L. Dexter. A Theory of Sensitized Luminescence in Solids. *J. Chem. Phys.*, 21:836–850, 1953.
  - [12] B.R. Masters. Paths to Förster’s resonance energy transfer (FRET) theory. *Eur. Phys. J. H*, 39:87–139, 2014.
  - [13] Augustine O. Allen. Yields of free ions formed in liquids by radiation. 1976.
  - [14] W.M. (Ed.) Haynes. *CRC Handbook of Chemistry and Physics (97th ed.)*. CRC Press, 2016.
  - [15] J. Allison et al. Recent developments in geant4. *Nucl. Instrum. Meth. A*, 835:186–225, 2016.
  - [16] J. Allison et al. Geant4 developments and applications. *IEEE Trans. Nucl. Sci.*, 53:270–278, 2006.
  - [17] S. Agostinelli et al. Geant4 - a simulation toolkit. *Nucl. Instrum. Meth. A*, 506:250–303, 2003.
  - [18] H. N. Tran et al. Review of chemical models and applications in geant4-dna: Report from the esa biorad iii project. *Med. Phys.*, 51:5873–5889, 2024.
  - [19] S. Incerti et al. Geant4-dna example applications for track structure simulations in liquid water: a report from the geant4-dna project. *Med. Phys.*, 45:e722–e739, 2018.
  - [20] M. A. Bernal et al. Track structure modeling in liquid water: A review of the geant4-dna very low energy extension of the geant4 monte carlo simulation toolkit. *Phys. Med.*, 31:861–874, 2015.
  - [21] S. Incerti et al. Comparison of geant4 very low energy cross section models with experimental data in water. *Med. Phys.*, 37:4692–4708, 2010.
  - [22] S. Incerti et al. The geant4-dna project. *Int. J. Model. Simul. Sci. Comput.*, 1:157–178, 2010.
  - [23] A. Garcia-Abenza et al. Evaluated electron scattering cross section dataset for gaseous benzene in the energy range 0.1-1000 ev. *Phys. Chem. Chem. Phys.*, 25:20510–20518, 2023.
  - [24] Ana I Lozano et al. Double and triple differential cross sections for single ionization of benzene by electron impact. *Int. J. Mol. Sci.*, 22:4601, 2021.
  - [25] Mohan Li, Ziyi Guo, Minfang Yeh, Zhe Wang, and Shaomin Chen. Separation of Scintillation and Cherenkov Lights in Linear Alkyl Benzene. *Nucl. Instrum. Meth. A*, 830:303–308, 2016.
  - [26] Ziyi Guo, Minfang Yeh, Rui Zhang, De-Wen Cao, Ming Qi, Zhe Wang, and Shaomin Chen. Slow Liquid Scintillator Candidates for MeV-scale Neutrino Experiments. *Astropart. Phys.*, 109:33, 2019.